

Crystal Structures of Tiotropium Bromide and Its Monohydrate in View of Combined Solid-state Nuclear Magnetic Resonance and Gauge-Including Projector-Augmented Wave Studies

EDYTA PINDELSKA,¹ LUKASZ SZELESZCZUK,² DARIUSZ MACIEJ PISKLAK,² ZBIGNIEW MAJKA,³ WACLAW KOLODZIEJSKI¹

¹Faculty of Pharmacy, Medical University of Warsaw, Department of Inorganic and Analytical Chemistry, Warsaw 02-093, Poland

²Faculty of Pharmacy, Medical University of Warsaw, Department of Physical Chemistry, Warsaw 02-093, Poland

³Pharmaceutical Company Adamed Ltd., Czosnow 05-152, Poland

Received 24 February 2015; revised 9 April 2015; accepted 15 April 2015

Published online 15 May 2015 in Wiley Online Library (wileyonlinelibrary.com). DOI 10.1002/jps.24490

ABSTRACT: Tiotropium bromide is an anticholinergic bronchodilator used in the management of chronic obstructive pulmonary disease. The crystal structures of this compound and its monohydrate have been previously solved and published. However, in this paper, we showed that those structures contain some major errors. Our methodology based on combination of the solid-state nuclear magnetic resonance (NMR) spectroscopy and quantum mechanical gauge-including projector-augmented wave (GIPAW) calculations of NMR shielding constants enabled us to correct those errors and obtain reliable structures of the studied compounds. It has been proved that such approach can be used not only to perform the structural analysis of a drug substance and to identify its polymorphs, but also to verify and optimize already existing crystal structures. © 2015 Wiley Periodicals, Inc. and the American Pharmacists Association *J Pharm Sci* 104:2285–2292, 2015

Keywords: solid state NMR; *ab initio* calculations; crystal structure; polymorphism; tiotropium bromide; GIPAW calculations; solid state characterization

INTRODUCTION

There is an increasing interest in the pulmonary route of administration for both local and systemically acting drugs or vaccines.¹ Inhaled aerosol therapy is capable of transferring the drug directly to the target organ, hence systemic drug levels can be reduced, whereas systemic exposure and adverse drug effects lowered.²

A very important decision in the development of inhaled medications is to select the best solid form of an active pharmaceutical ingredient (API) for particular pharmaceutical formulation. Each API polymorph has its specific physicochemical properties. Therefore, it is not easy to find the most appropriate solid form of API, taking into consideration possible polymorphism of pure API and of its solid derivatives (salts, solvates, and cocrystals). Various API polymorphs can crystallize in the different ways, forming crystals of different shapes and sizes. In some cases, aerosolization of a given polymorph can be very difficult because of its strong cohesive and adhesive properties.³ Besides, it may happen that over specific time metastable polymorphs undergo transformations into other forms during drug formulation or storage, spontaneously or as a result of interaction with excipients. Such transformations can greatly affect drug bioavailability.⁴

It should also be emphasized that for each polymorphic form of API, a separate patent protection can be obtained. This may be of a great importance for the fast-growing market of generic drugs. Furthermore, good quality crystal structures have to be

included in input files of some computational procedures used to determine solubility and other physicochemical properties of API.⁵

Therefore, accurate and reliable methods and procedures have to be developed to characterize API polymorphs and determine precisely their crystal structure. The characterization of API polymorphs can be accomplished by the powder X-ray diffraction (PXRD), or single-crystal X-ray diffraction, Fourier transform infrared spectroscopy, Raman spectroscopy, solid-state nuclear magnetic resonance (ssNMR), thermal analysis, and scanning electron microscopy; each of those analytical methods provides different information and has its own advantages and disadvantages. In many cases, ssNMR is the method of choice because of following important practical aspects.^{6–8} It can be used to analyze a final drug form without any need of special sample preparation, then ssNMR spectra do not usually pose problems with interpretation and the method can also be used for quantitative analysis. Any changes in the API structure (phase transitions) caused by molecular interactions or chemical bonding between API and associated excipients can easily be identified using the ssNMR spectra.

Tiotropium bromide (TIO), (1 α ,2 β ,4 β ,5 α ,7 β)-7-[(2-hydroxy-2,2-di-2-thienylacetyl)oxy]-9,9-dimethyl-3-oxa-9-azoniatricyclo[3.3.1.0^{2,4}]nonane bromide (Fig. 1) is an anticholinergic bronchodilator used in the management of chronic obstructive pulmonary disease. Unlike ipratropium and atropine that nonselectively block all three muscarinic receptors, TIO is more selective for the M₁ and M₃ receptors, from which it dissociates much more slowly. As a consequence, TIO is more potent bronchodilator than ipratropium, and has a much longer duration of action. A single dose of inhaled TIO produces bronchodilation that is sustained for 24 h or more.⁹ In a retrospective analysis of two studies performed in the United States,^{10,11} it was found that treatment with

Correspondence to: E. Pindelska (Telephone: +48-22-57-20-784; Fax: +48-22-57-20-784; E-mail: edyta.pindelska@wum.edu.pl)

This article contains Supplementary Materials available from the authors upon request or via the Internet at <http://onlinelibrary.wiley.com/>.

Journal of Pharmaceutical Sciences, Vol. 104, 2285–2292 (2015)

© 2015 Wiley Periodicals, Inc. and the American Pharmacists Association

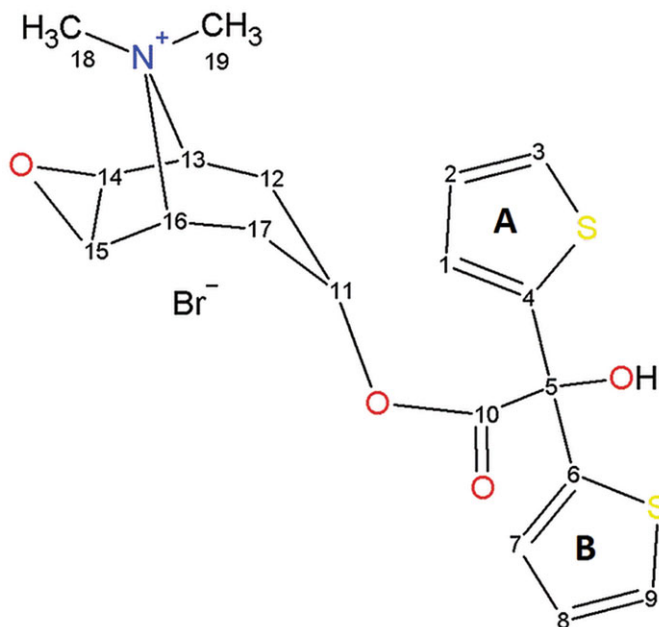


Figure 1. The structural formula and atom numbering of tiotropium bromide (TIO).

tiotropium reduced average total annual healthcare costs by approximately thousand US dollars per patient. This financial saving was entirely because of reduction in the hospitalization costs.¹² D'Souza et al.¹³ in their review article stated that treatment with tiotropium is undoubtedly more cost-effective than with ipratropium.

Tiotropium was synthesized and crystallized in various polymorphic forms,^{14,15} including hydrates and cocrystals, but only one of them, that is, tiotropium bromide monohydrate, is present in the commercially available drugs (Spiriva[®], Tiova[®]). In this study, we wish to focus on the anhydrous tiotropium bromide (TIOA) and its monohydrate (TIOH), for which four and three crystallographic information files, respectively, have been deposited in Cambridge Structural Database (CSD).¹⁶ However, only two of them contain complete structural data, the other five provide limited information without 3D atoms coordinations. Therefore, we can only make use of the two available structures with full crystallographic information: GUYGOX03 (structure of TIOA) and GUYGUD01 (structure of TIOH). It is worth mentioning that the other five structures have been assigned with the following comment from the CSD administration: “No reply to request for data.” The information about all of the deposited structures can be found in Table 1.

The main aims of our study were the following: (1) to assess the quality of the existing CSD crystal structures of TIOA and TIOH, (2) to develop a practical and nondestructive analytical procedure to distinguish TIO polymorphs, (3) to determine correct structures of TIO that can be used in the further analysis.

In this work, experimental and theoretical methods were applied in tandem: high-resolution solid-state ¹³C NMR spectroscopy and quantum mechanical calculations of NMR shielding constants. For NMR, cross-polarization (CP) under magic angle spinning (MAS) was employed.

Our principal intention was to verify the hypothesis that the quality of the published API crystal structure can be improved by using the density functional theory (DFT) method of ge-

ometry optimization for periodic systems,¹⁹ together with two experimental methods of structure quality verification: ssNMR and PXRD.

MATERIALS AND METHODS

Sample Preparation

Tiotropium bromide was obtained using a three-step synthesis according to known methods described previously.^{20–22} First, dimethyl glyoxalate was reacted with 2-thienylmagnesium bromide. Then, the obtained methyl di(2-thienyl)glycolate was subjected to transesterification with scopine hydrobromide in the presence of potassium carbonate to give scopine di(2-thienyl)glycolate. The final anhydrous tiotropium bromide was obtained by quaternisation of scopine di(2-thienyl)glycolate with methyl bromide. Monohydrate tiotropium bromide was prepared using previously published procedures.¹⁸

NMR Spectroscopy

The high-resolution ¹³C NMR spectra were collected at 298 K on a Bruker Avance 400 WB spectrometer using 100 MHz resonance frequency ($B_0 = 9.4$ T). The CP experiments²³ were performed with high-power proton decoupling using Bruker 7-mm MAS probe with zirconia rotors driven by dry air. The MAS rate was set at 7 kHz and the Hartmann-Hahn condition was matched using adamantane. We used a $\pi/2$ pulse of 4 μ s, and a recycle delay of 50 and 30 s for TIOA and TIOH, respectively (both optimized). Chemical shifts were referenced to TMS using glycine as an external secondary standard ($\delta_{CO} = 176.5$ ppm from TMS). The dipolar dephased experiments were carried out with dipolar filters to suppress the CP/MAS NMR signals from ¹³C nuclei strongly coupled to protons (CH and CH₂ groups). A 50- μ s delay before the FID acquisition results in the selective dephasing of magnetizations from methine and methylene groups was inserted. Conventional 1D and 2D NMR solution spectra in deuterated acetone were recorded on a Varian Unity Plus 300 MHz spectrometer (7.0 T, 298 K). The NMR spectra were processed with the ACD/SpecMenager NMR program.²⁴

Gauge-Including Projector-Augmented Wave CASTEP Calculations

The quantum chemical calculations of geometry, energy, and NMR shielding constants were carried out with the CASTEP program^{25,26} implemented in the Materials Studio 6.1 software.²⁷ Geometry optimizations and calculations of NMR chemical shielding were performed using the plane wave pseudopotential formalism and the Perdew–Burke–Ernzerhof exchange–correlation functional, defined within the generalized gradient approximation and the dispersion–interaction contributions were considered using the Tkatchenko–Scheffler method²⁸ for density functional theory dispersion correction. All the calculations were performed with ultrasoft pseudopotentials calculated on the fly; the quality of calculations was set to fine as implemented in the CASTEP standards. CASTEP default values for the geometry convergence criteria were used. The kinetic energy cutoff for the plane waves was set to 550 eV. Brillouin zone integration was performed using a discrete $1 \times 1 \times 1$ Monkhorst-Pack k-point sampling for a primitive cell. The computation of shielding tensors was performed using the gauge-including projector-augmented wave (GIPAW) method of Pickard et al.²⁹ Additional computational data can be found

Table 1. TIOA and TIOH Structures Formerly Deposited in Cambridge Structural Database

Form	REFCODE	Space Group	Cell Parameters (Å, °)	Volume (Å ³)	R-Factor (%)	Methods
TIOA	GUYGOX ¹⁴	Pbca	$a = 11.742$ $b = 17.796$ $c = 19.628$	4101.479	4.45	Single-crystal X-ray diffraction
	GUYGOX01 ¹⁴	P21/c	$a = 10.440$ $b = 11.326$ $c = 17.601$ $\beta = 104.99$	2010.382	5.87	Single-crystal X-ray diffraction
	GUYGOX02 ¹⁴	Pbca	$a = 15.550$ $b = 12.031$ $c = 20.893$	3908.705	3.87	Single-crystal X-ray diffraction
	GUYGOX03 ¹⁷	P21/c	$a = 10.434$ $b = 11.330$ $c = 17.633$ $\beta = 105.16$	2011.893	6.2	Powder X-ray diffraction
TIOH	GUYGUD ¹⁴	P21/c	$a = 9.939$ $b = 11.935$ $c = 18.558$ $\beta = 108.45$	2088.260	5.55	Single-crystal X-ray diffraction
	GUYGUD01 ¹⁸	P21/n	$a = 18.077$ $b = 11.971$ $c = 9.932$ $\beta = 102.69$	2096.859	6.2	Single-crystal X-ray diffraction
	GUYGUD02 ¹⁷	P21/n	$a = 18.077$ $b = 11.971$ $c = 9.932$ $\beta = 102.69$	2096.859	6.2	Single-crystal X-ray diffraction

in the Supplementary Materials (Tables 1S–4S). In the calculations, the experimental X-ray structures of cocrystals were used. Two approaches of geometry optimization have been performed. In the first one, hydrogen atoms positions were optimized, whereas heavy atoms and cell parameters were fixed to their experimental values. In the second one, all atom positions were optimized, whereas cell parameters were fixed to their experimental values. In the case of TIOH, the hydrogen atom positions were optimized, whereas in the case of TIOA, the hydrogen atoms had to be added, choosing their initial coordinates very carefully and then performing optimization of their positions. To compare the theoretical and experimental data, the calculated chemical shielding constants (σ_{iso}) were converted to chemical shifts (δ_{iso}), using the following equation: $\delta_{\text{iso}} = (\sigma_{\text{Gly}} + \delta_{\text{Gly}}) - \sigma_{\text{iso}}$, where σ_{Gly} and δ_{Gly} stand for the shielding constant and the experimental chemical shift, respectively, of the glycine carbonyl carbon atom (176.5 ppm).

PXRD Measurements

Powder X-ray diffraction patterns were obtained using Rigaku MiniFlex X-ray diffractometer, with Cu K α radiation and K β filter. Parameters of X-ray tubes were set at 30 kV and 15 mA. Divergence and scattering slits were set at 4.2°, and a receiving slit was set at 0.3 mm. Deflection of rays was detected with scintillation detector NaI. The $\theta/2\theta$ continuous scan at 1°/min with a step of 0.02° from 2.0° to 40° 2θ was used. Samples were prepared by pressing the solid in a quartz holder.

RESULTS AND DISCUSSION

The crystal structures of TIO polymorphs have been previously solved and deposited in CSD, and this has been described in

details in the *Introduction* section. However, analysis of the data from Table 1 raises the following crucial questions. (1) Are the structures deposited under the Refcodes GUYGOX01 and GUYGOX03 only the slightly different representations of the same polymorph? (2) What are the structural differences between the structures GUYGOX and GUYGOX02? Probably those questions could be answered if the missing structural data from the discussed files were known. As the files GUYGOX, GUYGOX01, GUYGOX02, GUYGUD, and GUYGUD02 contained no details on the atom positions, we could not perform required structural analysis of them and answer ourselves those questions.

Although TIO is a very popular API, any detailed structural studies of its polymorphs have not been reported yet. One of the reasons for this may be the relatively high cost of TIO. It is worth noticing that the standard dose of TIOH is 18 μg ³⁰; therefore, the quantity needed for the ssNMR measurements (about 50 mg) is equivalent to more than 2500 single therapeutic doses.

In order to perform ssNMR analysis of the differences between the TIO polymorphs, one needs good quality ¹³C spectra with properly assigned peaks. We started our interpretation by considering the solution spectrum of TIO. The peak assignments are presented in Tables 2 and 3. After that, we passed to the interpretation of the ¹³C CP/MAS NMR spectra of TIOA and TIOH (Figs. 2 and 3). This was carried out by reference to the solution chemical shifts (Tables 2 and 3) and by considering the dipolar dephased spectra. Dipolar dephasing experiments are usually very helpful in assigning the ¹³C CP/MAS NMR spectra of organic solids, as they display signals arising from ¹³C nuclei undergoing weak dipolar interactions with protons: from quaternary carbons (no adjacent protons) and from methyl carbons

Table 2. ^{13}C NMR Chemical Shifts (ppm) of TIOA

Group	Assignment	Solution Acetone-D6	ssNMR	GIPAW Values			
				Only H Optimized	$\Delta(\text{ssNMR-GIPAW})$	Full Optimization	$\Delta(\text{ssNMR-GIPAW})$
C	10	171.20	170.23	163.9	6.33	176	-5.77
C	4	147.86	151.83	157.2	-5.37	154.82	-2.99
C	6	147.86	151.83	199.29	-47.46	155.1	-3.27
CH	3	126.93	126	103.13	22.87	125.73	0.27
CH	9	126.93	126	123.2	2.8	126.17	-0.17
CH	2	127.62	126	116.32	9.68	126.96	-0.96
CH	8	127.62	126	106.97	19.03	126.83	-0.83
CH	1	126.72	122.2	113.8	8.4	120.15	2.05
CH	7	126.72	128.46	118.44	10.02	127.06	1.4
C	5	77.94	77.07	85.76	-8.69	79.09	-2.02
CH	13	66.22	66.75	54.16	12.59	66.21	0.54
CH	16	66.22	65.67	52.63	13.04	66.12	-0.45
CH	11	65.32	63.38	73.93	-10.55	62.23	1.15
CH ₃	18	56.79	55.61	56.58	-0.97	50.32	5.29
CH	14	55.00	54.46	53.08	1.38	56.62	-2.16
CH	15	55.00	55.61	53.57	2.04	57.15	-1.54
CH ₃	19	48.43	49.88	44.34	5.54	47.89	1.99
CH ₂	12	29.71	28.35	25.13	3.22	25.6	2.75
CH ₂	17	29.71	29.82	19.7	10.12	26.78	3.04
	R2			0.910		0.998	

Table 3. ^{13}C NMR Chemical Shifts (ppm) of TIOH

Group	Assignment	ssNMR	GIPAW Values			
			Only H Optimized	$\Delta(\text{ssNMR-GIPAW})$	Full Optimization	$\Delta(\text{ssNMR-GIPAW})$
C	10	170.5	165.99	4.51	176.67	-6.17
C	4	150.47	157.24	-6.77	152.54	-2.07
C	6	148.91	188.54	-39.63	151.24	-2.33
CH	3	125.8	117.93	7.87	124.96	0.84
CH	9	129.87	132.16	-2.29	130.51	-0.64
CH	2	129.87	130.59	-0.72	130.96	-1.09
CH	8	127.77	107.01	20.76	127.64	0.13
CH	1	122.1	126.06	-3.96	122.48	-0.38
CH	7	125.8	120.26	5.54	124.24	1.56
C	5	77.78	82.39	-4.61	78.98	-1.2
CH	13	66.51	65.33	1.18	65.29	1.22
CH	16	66.51	64.8	1.71	65.35	1.16
CH	11	63.71	65.05	-1.34	63.58	0.13
CH ₃	18	56.89	56.89	0	52.32	4.56
CH	14	54.73	56.35	1.62	55.45	0.72
CH	15	56.89	56.33	0.56	56.63	0.26
CH ₃	19	47.72	47.29	0.43	45.01	2.71
CH ₂	12	29.26	26.59	2.67	26.33	2.93
CH ₂	17	29.96	29.76	0.2	29.59	0.37
	R2		0.947		0.998	

Solution NMR data can be found in Table 2.

(group rotation).³¹ The dipolar-dephased spectra of TIOA and TIOH have been included in Supplementary Materials of this article.

The ssNMR peaks of TIOA and TIOH were generally narrow, thus indicative of a high structural order in the crystalline phase. Because of the apparent differences in the spectra of TIOA and TIOH, ssNMR enables simple and straightforward distinction between the samples of those two polymorphs. However, in order to find out what structural aspects of TIOA and TIOH are responsible for the differences in their NMR spectra (particularly evident in the 120–160 ppm region), it was neces-

sary to assign the peaks. Unfortunately, because of the signal overlapping, the proper assignment of the ^{13}C CP/MAS NMR peaks, based exclusively on the interpretation of the solution spectra and the solid-state dipolar-dephased spectra, was in this case infeasible.

Therefore, to achieve reliable assignment of the ^{13}C NMR signals from TIOA and TIOH, we have resorted to the GIPAW calculations of chemical shielding constants, preceded by the crystal structure optimization. In our recent article,³² we have proven that using a good quality crystal structure of organic solid compound, it is possible to calculate the NMR chemical

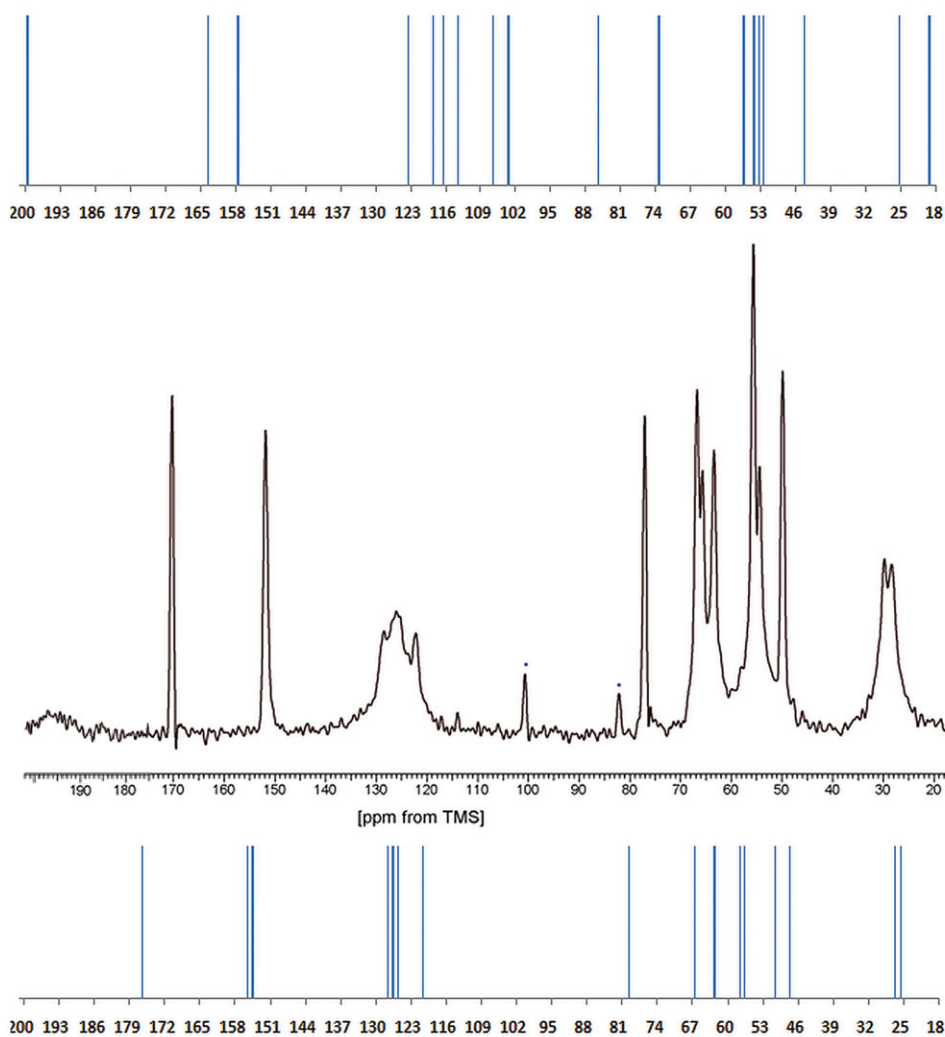


Figure 2. ^{13}C CP/MAS NMR spectra of the TIOA: calculated using the original CSD structure (top), experimental (middle), and calculated using our optimized structure (bottom).

shifts with very good precision. Therein, we have initially employed the standard procedure to optimize hydrogen atom positions with constrained positions of other atoms and cell parameters fixed to the experimental values. Such methodology has been successfully applied by us several times recently.^{8,32,33} In the present case, to create the input files for CASTEP calculations, we took advantage of the deposited crystal structures of TIOA (GUYGOX03) and TIOH (GUYGUD01). The obtained GIPAW results, collected in Tables 2 and 3, have then been used to simulate the ^{13}C NMR stick spectra, presented in Figures 2 and 3.

In both the TIOA and TIOH cases, we were amazed by the unexpectedly wrong results. The absolute values of the differences between the theoretically and experimentally obtained chemical shifts (Δ) were in some cases larger than 10 ppm, the largest one exceeded 40 ppm. The differences of such magnitude are extraordinary, even when performing the calculations of the isolated molecules that do not impose periodic boundary conditions. For both polymorphs, the worst results (the highest Δ) were observed for carbons of the thiophenyl rings. In order to explain such large differences, we have examined bond lengths

and bond angles in those rings and compared them with the experimental data from the crystal structure of the thiophene (Tables 4 and 5).³⁴ The thiophene reference data are adequate for such comparison. Certainly, some differences between the bond parameters of nonsubstituted and monosubstituted thiophene are expected, but the aromaticity of thiophene makes its structure rather insensitive to conformational changes resulting from substitution.

The bond length and bond angle values of the thiophenyl rings in the analyzed CSD structures of TIOA and TIOH were found dubious. The comparison of those values with the corresponding ones for thiophene confirmed our bad impression. For example, the C1-C2 bond length in TIOA (1.107 Å) was extremely small, more than 20% shorter than the corresponding parameter for thiophene. The bond angles did not agree with the experimental values as well, for example, C1-C2-C3 bond angle in TIOA was more than 20° larger than the corresponding one in thiophene.

Hence, it became clear to us that both studied CSD structures are wrong and contain some uncorrected major errors. Despite that nuisance, we did not give up and performed

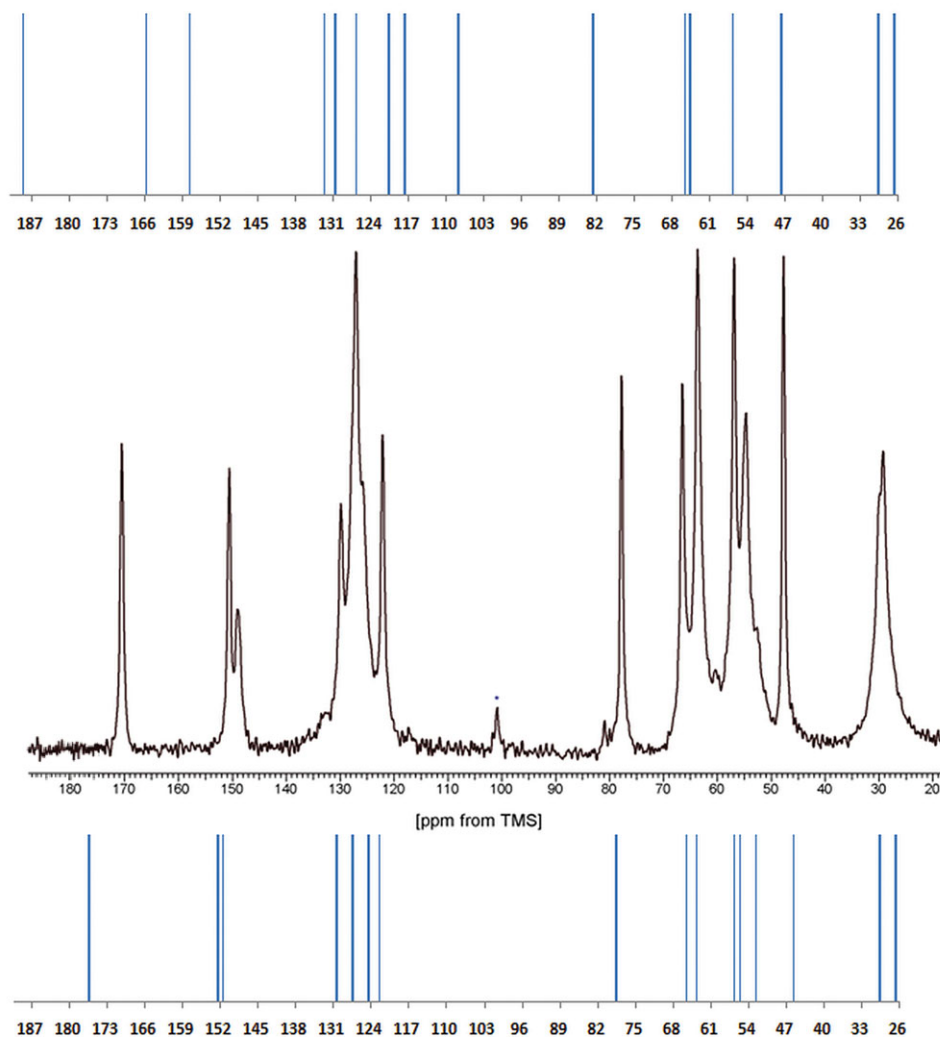


Figure 3. ^{13}C CP/MAS NMR spectra of the TIOH: calculated using the original CSD structure (top), experimental (middle), and calculated using our optimized structure (bottom).

full optimization of all the atoms positions. The fully optimized structures were then used to calculate the chemical shielding constants collected in Tables 2 and 3 and to simulate from them the ^{13}C NMR stick spectra, presented in Figures 2 and 3. Those fully optimized structures have been deposited by us as Supplementary Materials to this article.

After the full optimization of all the atom positions, the NMR shielding constants reached excellent agreement with the experimental values (e.g., R^2 for TIOA has increased from 0.910 to 0.998). Furthermore, the bond length and bond angle values after the full optimization were very close to the corresponding ones in thiophene, neglecting some small differences caused by the ring substituents (symmetry destruction of the nonsubstituted thiophene). The superimpositions of the original and optimized structures are shown in Supplementary Figure 1S.

To confirm that the structures generated by us after the full optimization are of superior quality and that they are real

representations of the studied polymorphs, we have simulated and compared PXRD patterns, computed using as the input files both nonoptimized and optimized structures of TIOA and TIOH. The results are presented in Figure 4. In both cases, a better agreement between the intensities of the reflexions has been achieved for the fully optimized structures; those differences were particularly evident in the case of TIOA. It is also worth to notice that our experimental PXRD patterns were almost identical with the corresponding ones presented in the US patents.

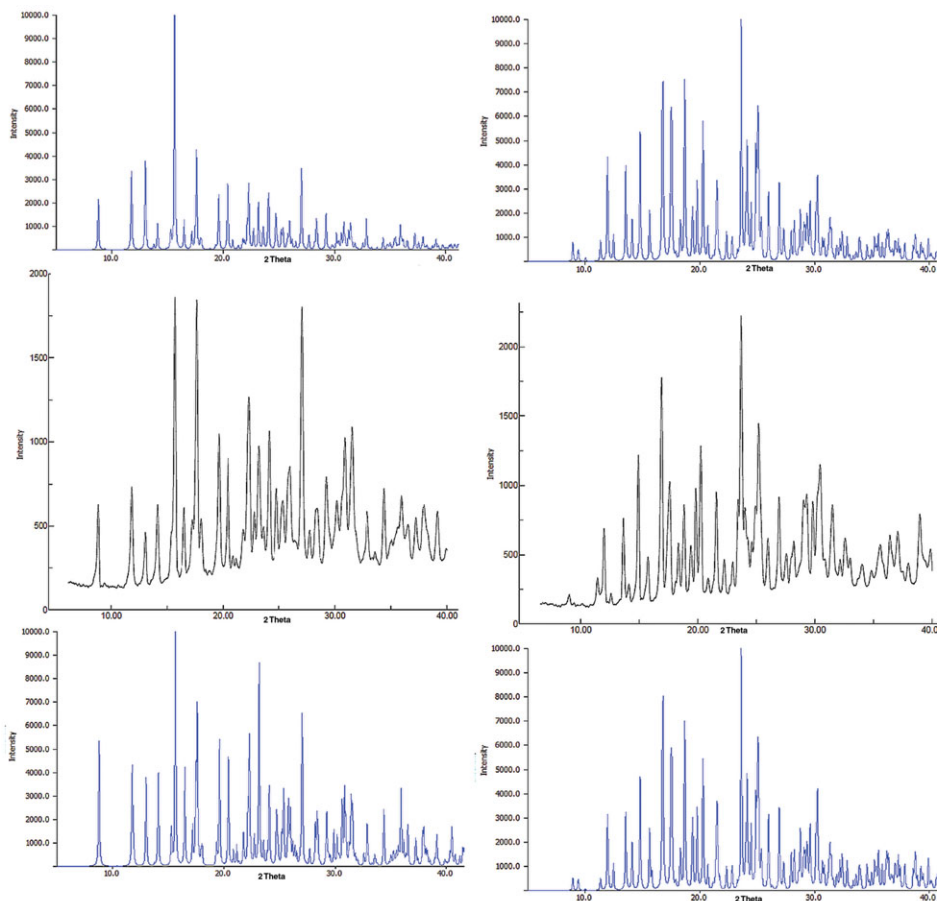
Not only simple comparison of the selected bond length and bond angle values, but also two experimental methods (PXRD and ssNMR) confirmed that the structures suggested by us (after optimization) are more accurate than the original ones. We have therefore proved that using the GIPAW calculations it is possible to correct the deposited crystal structures. As similar errors in the structures determination occurred twice (for TIOA and TIOH), they cannot be described as random.

Table 4. Selected Bond Lengths and Bond Angles in TIOA

Tiophenyl Ring	Selected Atoms	Bond Length (Å)/Bond Angle (°)		
		Only H Optimized	Full Optimization	Experimental Values for Thiophene ³⁴
A	S-C4	1.670	1.720	1.714
	C4-C1	1.588	1.379	1.370
	C1-C2	1.107	1.418	1.423
	C2-C3	1.410	1.377	1.370
	C3-S	1.784	1.717	1.714
	S-C4-C1	115.745	110.398	111.467
	C4-C1-C2	98.937	113.642	112.450
	C1-C2-C3	133.589	111.795	112.450
	C2-C3-S	103.551	111.677	111.467
	C3-S-C4	87.639	92.485	92.167
B	S-C6	1.668	1.722	1.714
	C6-C7	1.274	1.377	1.370
	C7-C8	1.464	1.422	1.423
	C8-C9	1.236	1.375	1.370
	C9-S	1.656	1.711	1.714
	S-C6-C7	113.069	110.965	111.467
	C6-C7-C8	108.808	112.768	112.450
	C7-C8-C9	114.120	112.270	112.450
	C8-C9-S	112.036	111.675	111.467
	C9-S-C6	91.523	92.319	92.167

Table 5. Selected Bond Lengths and Bond Angles in TIOH

Tiophenyl Ring	Selected Atoms	Bond Length (Å)/Bond Angle (°)		
		Only H Optimized	Full Optimization	Experimental Values for Thiophene ³⁴
A	S-C4	1.686	1.719	1.714
	C4-C1	1.398	1.379	1.370
	C1-C2	1.429	1.422	1.423
	C2-C3	1.337	1.374	1.370
	C3-S	1.700	1.711	1.714
	S-C4-C1	113.240	111.245	111.467
	C4-C1-C2	108.795	112.464	112.450
	C1-C2-C3	114.017	112.333	112.450
	C2-C3-S	112.446	111.772	111.467
	C3-S-C4	91.498	92.176	92.167
B	S-C6	1.676	1.724	1.714
	C6-C7	1.571	1.380	1.370
	C7-C8	1.099	1.420	1.423
	C8-C9	1.423	1.376	1.370
	C9-S	1.759	1.712	1.714
	S-C6-C7	115.874	110.483	111.467
	C6-C7-C8	99.288	113.100	112.450
	C7-C8-C9	132.944	112.303	112.450
	C8-C9-S	104.039	111.494	111.467
	C9-S-C6	87.643	92.602	92.167

**Figure 4.** Powder X-ray diffractograms of the TIOA (left) and TIOH (right): calculated using the original structure (top), experimental (middle), and calculated using our optimized structure (bottom).

CONCLUSIONS

On the basis of the solution ^{13}C NMR spectra, the dipolar-dephased NMR experiments and the GIPAW calculations we have assigned ^{13}C CP/MAS NMR spectra of TIOA and TIOH. We have demonstrated that looking at the differences in the spectra of those polymorphs it is easy to distinguish them using ssNMR spectroscopy. The NMR chemical shifts calculated on the basis of previously published crystal structures of TIOA and TIOH did not agree with the experimental values. As the GIPAW calculations are very sensitive to the atom positions, those divergent results indicated that the analyzed CSD structures contain some major errors. Those errors were identified and corrected by us using the BFGS method of geometry optimization employed within the CASTEP code. The accuracy of the optimized structures was confirmed using the ssNMR and PXRD methods. Therefore, we have shown that this approach can be used not only to perform the structural analysis of a drug compound and to easily differentiate its polymorphs, but also to verify and improve its already published crystal structure.

REFERENCES

- de Boer AH, Hagedoorn P. 2015. The role of disposable inhalers in pulmonary drug delivery. *Expert Opin Drug Deliv* 12:143–157.
- Rau JL. 2005. The inhalation of drugs: Advantages and problems. *Respir Care* 50:367–382.
- Ikegami K, Kawashima Y, Takeuchi H, Yamamoto H, Isshiki N, Momose D, Ouchi K. 2002. Improved inhalation behavior of steroid KSR-592 in vitro with Jethaler by polymorphic transformation to needle-like crystals (beta-form). *Pharm Res* 19:1439–1445.
- Bauer J, Spanton S, Henry R, Quick J, Dziki W, Porter W, Morris J. 2001. Ritonavir: An extraordinary example of conformational polymorphism. *Pharm Res* 18:859–866.
- Palmer DS, Llinàs A, Morao I, Day GM, Goodman JM, Glen RC, Mitchell JB. 2008. Predicting intrinsic aqueous solubility by a thermodynamic cycle. *Mol Pharm* 5:266–279.
- Pindelska E, Dobrzycki L, Woźniak K, Kolodziejski W. 2011. Polymorphism of crystalline 4-amino-2-nitroacetanilide. *Cryst Growth Des* 11:2074–2083.
- Zielińska-Pisklak M, Pisklak DM, Wawer I. 2012. Application of ^{13}C CPMAS NMR for qualitative and quantitative characterization of carvedilol and commercial formulations. *J Pharm Sci* 101:1763–1772.
- Pindelska E, Szeleszczuk L, Pisklak DM, Mazurek A, Kolodziejski W. 2015. Solid-state NMR as an effective method of polymorphic analysis: Solid dosage forms of clopidogrel hydrogensulfate. *J Pharm Sci* 104:106–113.
- Barnes PJ. 2000. The pharmacological properties of tiotropium. *Chest* 117:63S–66S.
- Casaburi R, Mahler DA, Jones PW, Wanner A, San PG, ZuWallack RL, Menjoge SS, Serby CW, Witek Jr. T. 2002. A long-term evaluation of once-daily inhaled tiotropium in chronic obstructive pulmonary disease. *Eur Respir J* 19:217–224.
- Friedman M, Menjoge SS, Anton SF, Kesten S. 2004. Healthcare costs with tiotropium plus usual care versus usual care alone following 1 year of treatment in patients with chronic obstructive pulmonary disorder (COPD). *Pharmacoeconomics* 22:741–749.
- Rice KL, Kunisaki KM, Niewoehner DE. 2007. Role of tiotropium in the treatment of COPD. *Int J Chron Obstruct Pulmon Dis* 22:95–105.
- D'Souza AO, Smith MJ, Miller LA, Kavookjian J. 2006. An appraisal of pharmaco-economic evidence of maintenance therapy for COPD. *Chest* 129:1693–1708.
- Pop M, Sieger P, Cains PW. 2009. Tiotropium fumarate: An interesting pharmaceutical co-crystal. *J Pharm Sci* 98:1820–1834.
- Diulgheroff N, Scarpitta F, Pontiroli A, Kovacsne-Mezel A, Aronhime J, Jegorov A. 2007. Novel forms of tiotropium bromide and processes for preparation thereof. Patent WO2007/075858 A2.
- Allen FH. 2002. The Cambridge Structural Database: A quarter of a million crystal structures and rising. *Acta Cryst B* 58:380–388.
- Sieger P, Werthmann U. 2003. Crystalline anticholinergic processes for preparing it and its use for preparing a pharmaceutical composition. Patent US6608055 B2.
- Banholzer R, Sieger P, Kulinna Ch, Trunk M, Graulich M, Specht P, Meissner H, Mathes A. 2004. Crystalline tiotropium bromide monohydrate, processes for the preparation thereof, and pharmaceutical compositions. Patent US6777423 B2.
- Head JD, Zerner MC. 1985. A Broyden-Fletcher-Goldfarb-Shanno optimization procedure for molecular geometries. *Chem Phys Lett* 122:264–270.
- Nyberg K, Östman B, Wallerberg G. 1970. Investigations of dithienylglycolic esters. I. Preparation of methyl dithienylglycolates. Magnetically nonequivalent protons in dithienylglycolates. *Acta Chim Scand* 24:1590–1596.
- Busolli J, Diulgheroff N, Pontiroli A, Scarpitta F, Volonte R. 2008. Scopine salts and their use in processes for the preparation of n-demethyl-tiotropium and tiotropium bromide. Patent WO2008008376 A8.
- Banholzer R, Bauer R, Reichl R. 1997. Esters of thienyl carboxylic acids and amino alcohols and their quaternization products. Patent US5610163.
- Pines A, Gibby MG, Waugh JS. 1973. Proton-enhanced NMR of dilute spins in solids. *J Chem Phys* 59:569–590.
- ACD/SpecMenager, version 10.08, Advanced Chemistry Development, Inc., 2007, <http://www.acdlabs.com/>.
- Segall MD, Lindan PJD, Probert MJ, Pickard CJ, Hasnip PJ, Clark SJ, Payne MC. 2002. First-principles simulation: Ideas, illustrations and the CASTEP code. *J Phys Condens Matter* 14:2717–2744.
- Yates JR, Pickard CJ, Mauri F. 2007. Calculation of NMR chemical shifts for extended systems using ultrasoft pseudopotentials. *Phys Rev B* 76:024401.
- Materials Studio v 6.1 Copyright Accelrys Software Inc. 2013, <http://accelrys.com/products/materials-studio/>.
- Tkatchenko A, Scheffler M. 2009. Accurate molecular van der Waals interactions from ground-state electron density and free-atom reference data. *Phys Rev Lett* 102:073005.
- Pickard CJ, Mauri F. 2001. All-electron magnetic response with pseudopotentials: NMR chemical shifts. *Phys Rev B* 63:2451011–2451013.
- Pearson M. 2004. Chronic obstructive pulmonary disease: National clinical guideline on management of chronic obstructive pulmonary disease in adults in primary and secondary care. *Thorax* 59:1–232.
- Guilbaud JB, Clark BC, Meehan E, Hughes L, Saiani A, Khimiyak YZ. 2010. Effect of encapsulating a pseudo-decapeptide containing arginine on PLGA: A solid-state NMR study. *J Pharm Sci* 99:2681–2696.
- Pindelska E, Sokal A, Szeleszczuk L, Pisklak DM, Kolodziejski W. 2014. Solid-state NMR studies of theophylline co-crystals with dicarboxylic acids. *J Pharm Biomed Anal* 100:322–328.
- Mazur L, Jarzębska KN, Kamiński R, Woźniak K, Pindelska E, Zielińska-Pisklak M. 2014. Substituent and solvent effects on intermolecular interactions in crystals of N-acylhydrazones derivatives: Single-crystal X-ray, solid-state NMR, and computational studies. *Cryst Growth Des* 14:2263–2281.
- Bak B, Christensen D, Hansen-Nygaard L, Rastrup-Andersen J. 1961. The structure of thiophene. *J Mol Spectr* 7:58–63.